Microstructure and Crystallographic Texture Characterization of Friction Stir Welded Thin AA2024 Aluminum Alloy

M. Alvand [1], M. Naseri [2], E. Borhani [3] and H. Abdollah-Pour [*1]

* *habd@semnan.ac.ir*

Received: November 2017 Accepted: February 2018

[1] Faculty of Materials and Metallurgical Engineering, Semnan University, Semnan, Iran.

[2] Department of Materials Science and Engineering, Faculty of Engineering, Shahid Chamran University of Ahvaz, Ahvaz, Iran.

[3] Department of Nano Technology, Nano Materials Group, Semnan University, Semnan, Iran.

DOI: 10.22068/ijmse.15.1.53

Abstract: *Friction stir welding (FSW) is a promising technique to join aluminum alloys without having problems encountered during fusion welding processes. In the present work, the evolution of microstructure and texture in friction stir welded thin AA2024 aluminum alloy were examined by electron backscattered diffraction (EBSD) technique. The sheets with 0.8 mm thickness were successfully welded by friction stir welding at the tool rotational speeds of 500, 750, and 1000 rpm with a constant traverse speed of 160 mm/min. EBSD revealed that stir zones exhibited equiaxed recrystallized grains and the grain size increased with increasing the tool rotation rate. The fraction of high angle grain boundaries and mean misorientation angle of the boundaries in the FSW joints at 500 rpm were 63.6% and 24.96°, respectively, which were higher than those of the sample welded at 1000 rpm (53.6% and 17.37°). Crystallographic texture results indicated that the Cube {001}<100> and S {123}<634> textures in base metal gradually transformed in to Copper {112}<111> texture. It was found that with increasing the tool rotation rate, the intensity of Cube {001}<100>, Y {111}<112>, S {123}<634>, and Dillamore {4 4 11}<11 11 8> texture orientations increased and the intensity of Brass {011}<211> texture orientation decreased.*

Keywords: *Aluminum Alloy, Friction Stir Welding, Electron Backscatter Diffraction, Microstructure, Crystallographic Texture.*

1. INTRODUCTION

Aluminum alloys, which are normally difficult to weld with conventional welding methods, are used widely in marine, aerospace, automotive, electrical and refrigeration industries. Friction stir welding (FSW) is a solid-state joining method which was firstly invented by The Welding Institute (TWI, Cambridge, UK) in 1991 [1]. FSW involves a non-consumable cylindrical tool with a specially designed pin and shoulder, rotating at a very high speed and plunging into adjacent edges of the metal pieces, thereby joining them. The basic principle of FSW is shown in Fig. 1 [2]. The two workpieces to be welded are kept into contact and clamped. When the rotating tool is inserted into the workpieces, the resulted frictional heating brings the two workpieces to a plasticized state. By tool translating along the joint line, the material is stirred and forged from the front face of the tool to the trailing face, where it cools down to form a solid state weld. During this solid state welding process, problems such as liquation cracking, porosity, entrapment of oxide films, strength loss due to welding and distortion that take place during other welding process do not occur. Furthermore, the process does not involve any use of filler metal and therefore, in contrast to fusion welding, the compatibility of composition is not an issue in FSW [3-5].

Usually in the friction stir welded joints of aluminum alloys, four distinct zones with different characteristics can be specified, the stir zone (SZ), the thermomechanically affected zone (TMAZ), the heat affected zone (HAZ), and the base material (BM) [6, 7]. Investigating microstructure and texture evolutions during FSW is of great importance. The related phenomena are deformation and dynamic recrystallization that affect performance mechanical properties of welded workpiece [8-10].

[DOI: 10.22068/ijmse.15.1.53]

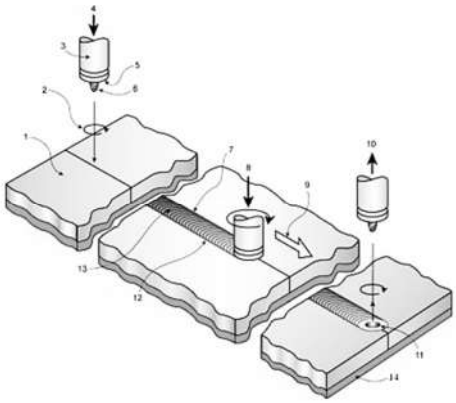

Fig. 1. Schematic illustration of the friction stir welding process in this study [2].

For the friction stir welding joints, microstructural evolutions, texture and the mechanical properties of various zones in friction stir welded joints are determined by the material flow behavior and heat input conditions [11]. Material flow and heat input are strictly influenced by friction stir welding parameters such as rotation rate, welding speed, tool geometry, and joint design. Babu et al. [12] and Zhang et al. [13] found that mechanical properties of FSW AA2219-T651 and FSW AA2219-T6 joints decreases by increasing the rotation rate or decreasing the welding speed. Suhuddin et al. [14] had studied microstructure and texture evolution during friction stir welding of thin 6016 aluminum alloy. They reported the formation of a simple shear texture ({112}<110>) having a characteristic Cube {100}<100> texture in the stir zone. Friction stir welding of Ti–6Al–4V alloys were conducted by Liu et al. [15, 16] team and it was claimed that the microstructure of the weld zone exhibited a mixture of the equiaxed grains and lamellar structure. In addition, they also pointed out that the mechanical properties of the joints increased with decreasing the heat input. Therefore, the effect of the friction stir welding parameters on the joint properties is completely different in different alloys, and in order to obtain high quality friction stir welding joints, optimizing the FSW parameters is of great importance.

The AA2024 aluminum alloy is a strategic alloy with outstanding properties and widespread application in automobile, aerospace, and defense applications. The aim of this research was to determine the effect of friction stir welding process on the grain structure and crystallographic texture evolution of thin AA2024 sheets by electron backscatter diffraction (EBSD) method.

2. EXPERIMENTAL PROCEDURES

Annealed AA2024 aluminum alloy sheet was supplied as 0.8 mm thick sheet 200 mm long and 50 mm wide with chemical composition given in Table 1. A FSW tool made of H13 hot work tool steel with a shoulder diameter of 20 mm, a pin diameter of 6 mm and a pin length of 0.5 mm was used (Fig. 2). The back tilting angle of the tool was 4° during FWS process. The tool rotation rate was changed in a range from 500 rpm to 1000 rpm while tool traverse speed was kept constant at 160 mm/min.

EBSD was carried out in a field-emission scanning electron microscope (FE-SEM, Philips XL30S) in order to characterize microstructure and crystallographic feature of the FSW joints. The section of the specimen was prepared by mechanically and then electrolytically polishing in a 30% HNO3 and 70% CH3OH solution at approximately 30 °C with a voltage of 15 V. All the microstructures were observed from the transverse direction (TD) of the sheets. The SEM system was operated at 15 kV. The EBSD measurements (the central thickness region) carried out with a step size of 50 nm and the obtained data was analyzed by TSL-OIMTM analysis software. Orientation distribution functions were calculated using Bunge's series expansion method, with an expansion degree

[DOI: 10.22068/ijmse.15.1.53]

Table 1. Chemical composition of 2024 aluminum alloy (wt.%).

Al	Cu	Cr	Fe	Mg	Mn	Si	Ti	Zn	V	Ga
92.99	4.50	0.01	0.25	1.50	0.55	0.10	0.02	0.05	0.02	0.01

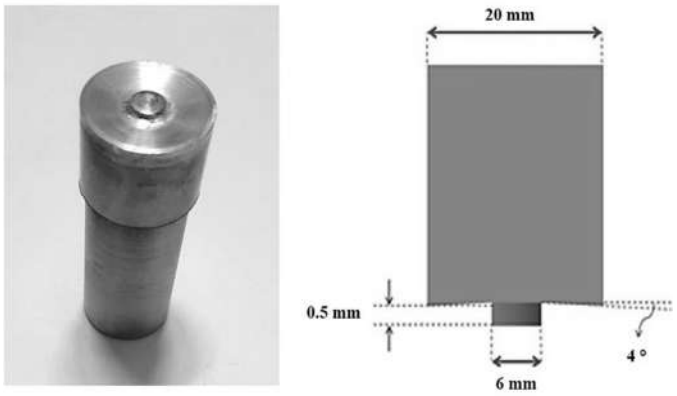

Fig. 2. Typical drawing of the tool applied for friction stir welding process.

of lmax = 22 in Euler space. In order to obtain appropriate EBSD observation for texture evolution, the relatively large area of the specimen's section having more than 500 grains was considered.

Vickers microhardness profiles were measured on the cross section perpendicular to the welding direction along the mid-thickness of the plates using a computerized Buehler hardness tester with a 100 g load and 10 s.

3. RESULTS AND DISCUSSION

3. 1. Microstructural Investigation

The EBSD microstructure photograph map of the 2024 aluminum alloy is displayed in Fig. 3. The orientations of each grain in this figure as depicted by the unit triangle are shown by different colors in color map. In the grain

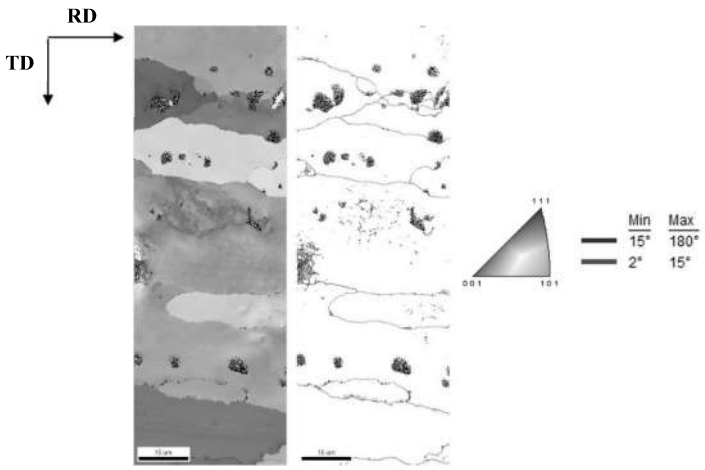

Fig. 3. OIM photograph and grain boundary map of the 2024 aluminum alloy.

[DOI: 10.22068/ijmse.15.1.53]

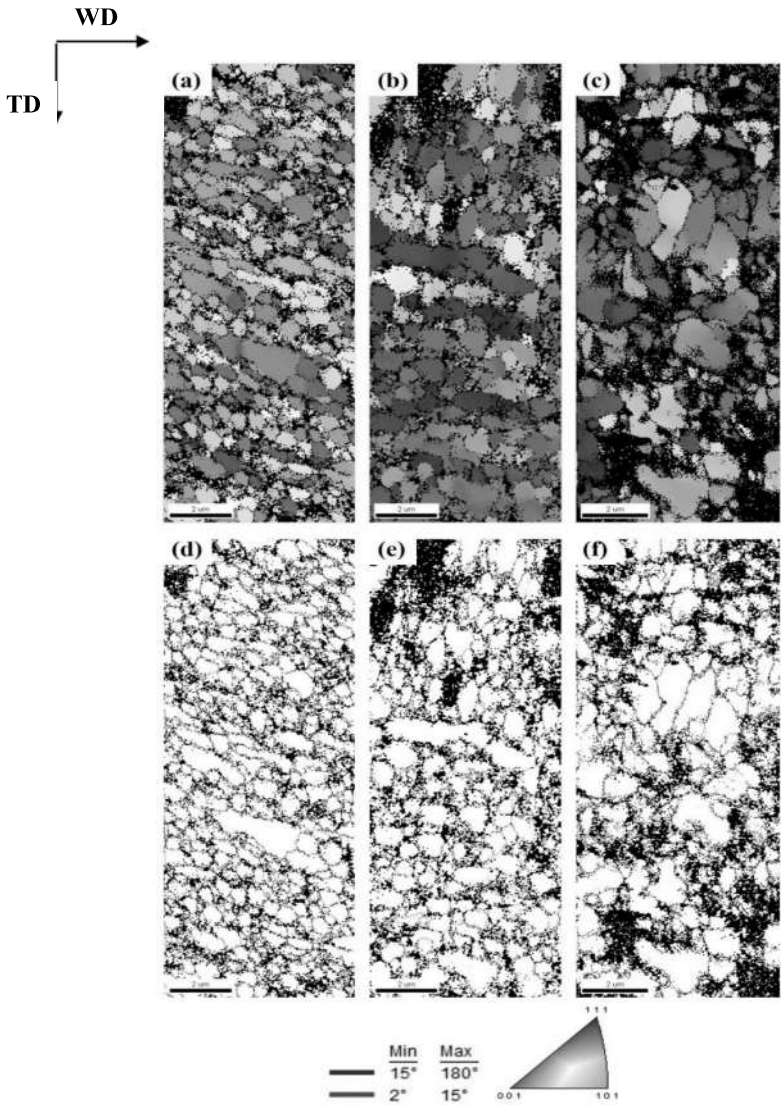

Fig. 4. OIM photographs and grain boundary maps of stir zone of FSW joints at (a and d) 500 rpm–160 mm/min, (b and e) 750 rpm–160 mm/min, and (c and f) 1000 rpm–160 mm/min.

boundary maps, high angle grain boundaries (HAGBs) low angle grain boundaries (LAGBs) with misorientation greater than 15° and misorientation between 2° and 15° are indicated by green and red lines, respectively. The boundaries having misorientation less than 2° are not taken in to account in order to improve the inaccuracy measurement of the EBSD. The initial grain size, calculated using the linear intercept method in the normal direction of the elongated grains, before the friction stir welding trials is about 30 μm.

The microstructure of the stir zone obtained at various tool rotation rates is shown in Fig. 4. Also, Fig. 5 shows the grain diameter distributions for the stir zone of FSW joints. The microstructure morphology in all stir zones exhibited inhomogeneous distribution along the plate thickness direction. The orientation color maps of nugget reveal that fine and equiaxed grains are formed in this zone. Also, OIM photographs exhibit a substantial fraction of

[DOI: 10.22068/ijmse.15.1.53]

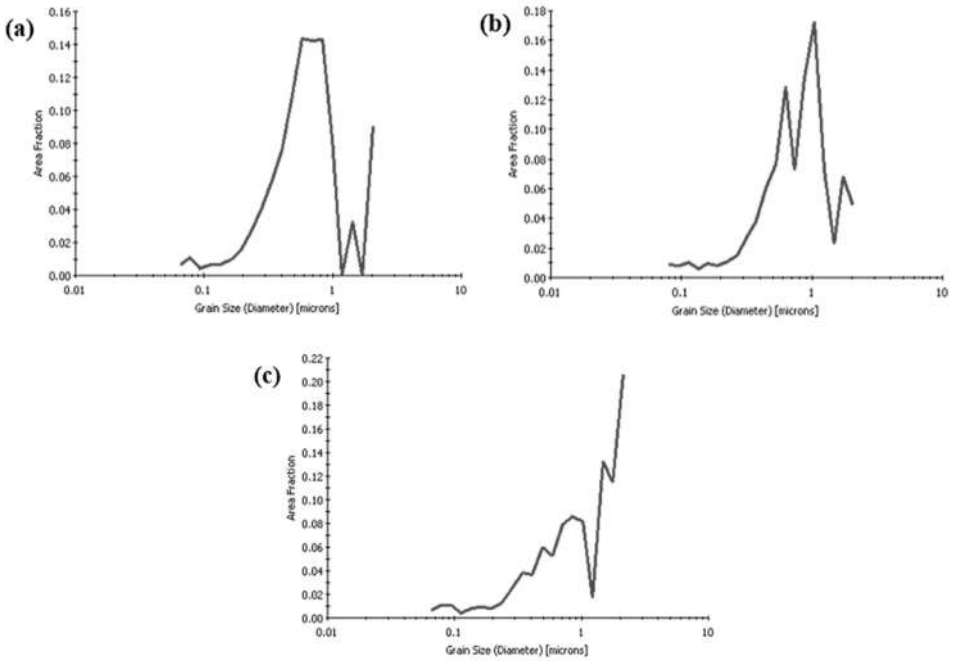

Fig. 5. Grain diameter distributions (from OIM software) of stir zone of FSW joints at (a) 500 rpm–160 mm/min, (b) 750 rpm–160 mm/min, and (c) 1000 rpm–160 mm/min.

unindexed pixels, primarily located at the grain boundaries. During friction stir welding process, fine and equiaxed grains are formed due to the mechanical mixing of materials and the thermal cycle [17, 18]. At a constant welding speed of 160 mm/min, with increasing the rotation rate from 500 to 1000 rpm the grain sizes in the stir zones increased from 0.5 to 1.8 μm. The correspondence between the color and the crystallographic orientation is indicated in the stereographic triangle. The color maps of the FSW specimen (1000 rpm–160 mm/min) indicate that preferred orientation develops by friction stir welding process, as particular colors become dominant in the orientation color maps. The normal direction (ND) orientation color map of the FSW specimen (1000 rpm–160 mm/min) demonstrates purple color as dominant color corresponding to <111>//ND.

The fraction of high angle grain boundaries ( ) and the mean misorientation angle of the boundaries ( ) were calculated from the EBSD data of each specimen (Fig. 6). At a constant welding speed of 160 mm/min, the and the for the FSW sample processed to 500 rpm are 63.60% and 24.96°, respectively, while for those of 1000 rpm are 53.60% and 17.37°, respectively. The EBSD analysis shows that the large grains of the 2024 aluminum alloy turn to fine grains and a large number of grain boundaries become high angle during friction stir welding process. Our results is consistent with previous study which indicated that the dislocations produced by deformation process are drawn to subgrain boundaries, which resulted in the increase of misorientation of LAGBs, and LAGBs transformed into HAGBs, leading to fine microstructure [19, 20].

Since the microstructure in the stir zone is strongly influenced by the friction heat flow, it is considered as a very important factor for friction stir welding process. Kim et al. [21] suggested the following equation describing the heat input from the shoulder during friction stir welding process:

$$q = \frac{4}{3}\pi^2 \mu P \omega R^3 \quad (1)$$

[DOI: 10.22068/ijmse.15.1.53]

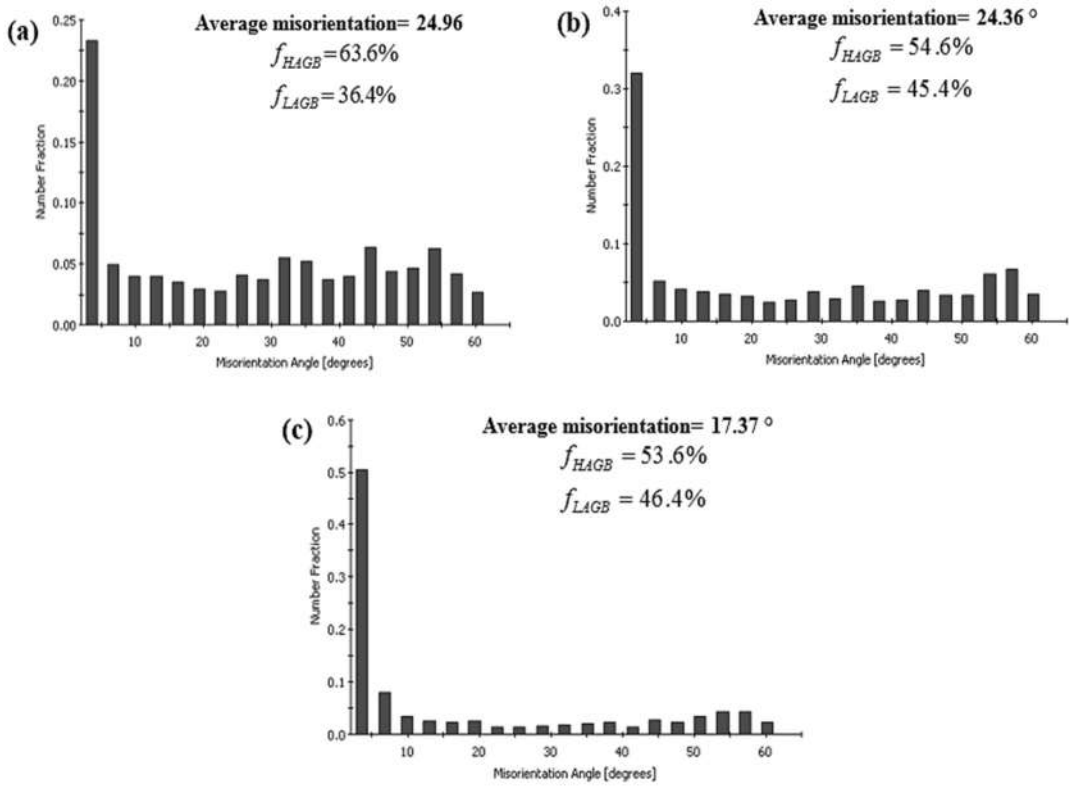

Fig. 6. The misorientation angle distribution of stir zone of FSW joints at (a) 500 rpm–160 mm/min, (b) 750 rpm–160 mm/min, and (c) 1000 rpm–160 mm/min.

where q, μ, P, ω, and R are heat input, friction coefficient, pressure, rotation rate, and the radius of the shoulder, respectively. The Eq. (2) is obtained by considering the welding speed.

$$Q = \frac{\alpha q}{V} = \frac{4}{3}\pi^2 \frac{\alpha \mu P \omega R^3}{V} \quad (2)$$

where Q, α, and V are the heat input per unit length, heat input efficiency, and the welding speed, respectively. Since the welding condition is the same, α, μ, P, and R are assumed to be constant, and only the ω and V are variable. Therefore Q can be expressed by

$$Q = \beta \frac{\omega}{V} \quad (3)$$

Increasing the tool rotation rate or decreasing the welding speed leads to increase in the heat input as shown in Eq. (3). Therefore, with higher tool rotation rate, the increased heat input lead to an increase in the size of recrystallized grains [10, 13].

3. 2. Crystallographic Texture

Crystallographic texture is an important factor to determining the anisotropic response of a material under deformation. The FSW processed materials are intrinsically related to the presence of different grains in the microstructure leading to various texture components. The ODFs are presented as plots of constant φ_2 sections with intensity contours in Euler space defined by the Euler angles φ_1, Φ, and φ_2. The ideal orientations of texture components in FCC materials are shown for the 0 and 45° ODF sections in Fig. 7 and Table 2.

[DOI: 10.22068/ijmse.15.1.53]

Table 2. Euler angles and Miller indices for important texture components in FCC materials.

Texture component	Miller indices	Euler angles			Fiber
		φ_1	ϕ	φ_2	
Cube	{001}<100>	0	0	0	Cube-Goss/θ
Rotated cube	{001}<110>	45	0	0	θ
Goss	{011}<100>	0	45	0	Cube-Goss/α/τ
Rotated goss	{011}<011>	90	45	0	α
Goss twin	{113}<332>	90	25	45	τ
Brass	{011}<211>	35	45	0	α/β
Goss/brass	{011}<115>	16	45	0	α
A	{011}<111>	55	45	0	α
Y	{111}<112>	90	55	45	γ/τ
E	{111}<011>	60	55	45	γ
Copper	{112}<111>	90	35	45	τ/β
Rotated copper	{112}<011>	0	35	45	-
Copper twin	{554}<115>	90	74	45	τ
Dillamore	{4 4 11}<11 11 8>	90	27	45	τ
S	{123}<634>	59	37	63	β
S/brass	{414}<234>	49	40	75	β

In order to have a better understanding and quantitative analysis of texture development during the friction stir welding process, the ODFs were analyzed using the EBSD data. The ODF plots separate the components partially overlapping in the pole figures (PFs), thus they facilitate a more unambiguous comparison of the individual components and fibers [20, 23, 24]. Fig. 8 illustrates the ODFs of the 2024 aluminum alloy and stir zone of FSW joints. As shown in Fig. 8(a), the textural components in the initial sample can be characterized as the Cube {001}<100>, Brass {011}<211>, and S {123}<634> having the intensity of 5.5 × R, 3.2 × R, and 26.5 × R, respectively. After FSW process at 500 rpm–160 mm/min (Fig. 8(b)), the Copper {112}<111> and Y {111}<112> with maximum intensity of 3.2 × R and 9.5 × R which were typical shear texture component are created. As shown in Fig. 8(c), increasing the rotation rate from 500 to 750 rpm, the Cube {001}<100>, Copper {112}<111>, and Y {111}<112>

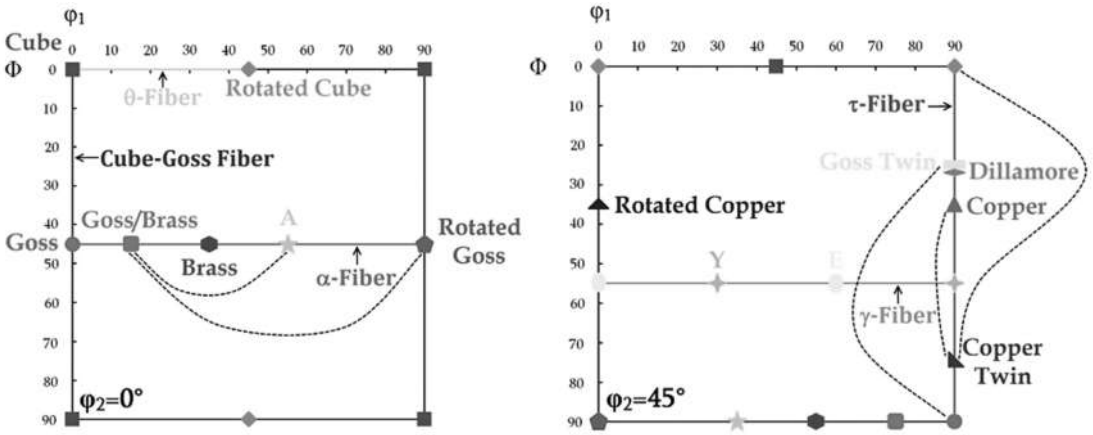

Fig. 7. Schematic illustration of the important texture components in FCC materials. The dashed lines depict twin relationships [22].

[DOI: 10.22068/ijmse.15.1.53]

components disappeared and the Goss {011}<100> and Brass {011}<211> components became stronger. Also, increasing the rotation rate from 750 to 1000 rpm (Fig. 8(d)), the Cube {001}<100>, S {123}<634> and Dillamore {4 4 11}<11 11 8> appeared again and the intensity of the Brass {011}<211> decreased to 3.5 × R.

The Cube {001}<100> texture component is metastable in the friction stir welding process, the preexisting Cube grains will form long, thin Cube orientated regions (Cube bands). Some researchers express that the grain size in the Cube bands is larger than elsewhere. This makes them as effective nucleation sites for recrystallization [25]. In the annealing texture of FCC materials, the Cube {001}<100> component is the dominant texture component made by the combination of the nucleation and growth advantages [26]. During friction stir welding process, the stir zone experienced intense plastic deformation and thermal exposure with the peak temperatures up to 0.6–0.95 TM. Also, formation of shear texture suggests the possibility of some restoration process (recovery, recrystallization, and grain growth) [14, 27].

Due to high stacking fault energy of aluminum alloys (166 mJm^{-2}), the recovery is easy to occur. The differences in texture evolution can be attributed to occurrence of recrystallization and grain growth in the material because the recovery does not alter the texture of the materials, hence the recovery can take place at all samples (Fig. 4). Based on the obtained results, it can be said that at the early stage of recrystallization during friction stir welding process, the Goss {011}⟨100⟩ and Copper {112}<111> texture components are evolved and the fraction of grains with α-fiber and τ-fiber orientations is decreased and the shear texture is increased. Afterwards, during the grain growth stage, the intensity of α-fiber and τ-fiber is increased and the shear texture is decreased.

3. 3. Mechanical Properties

Fig. 9 shows the hardness profiles of the FSW joints along the mid-thickness of the transverse section at different parameters. The hardness in

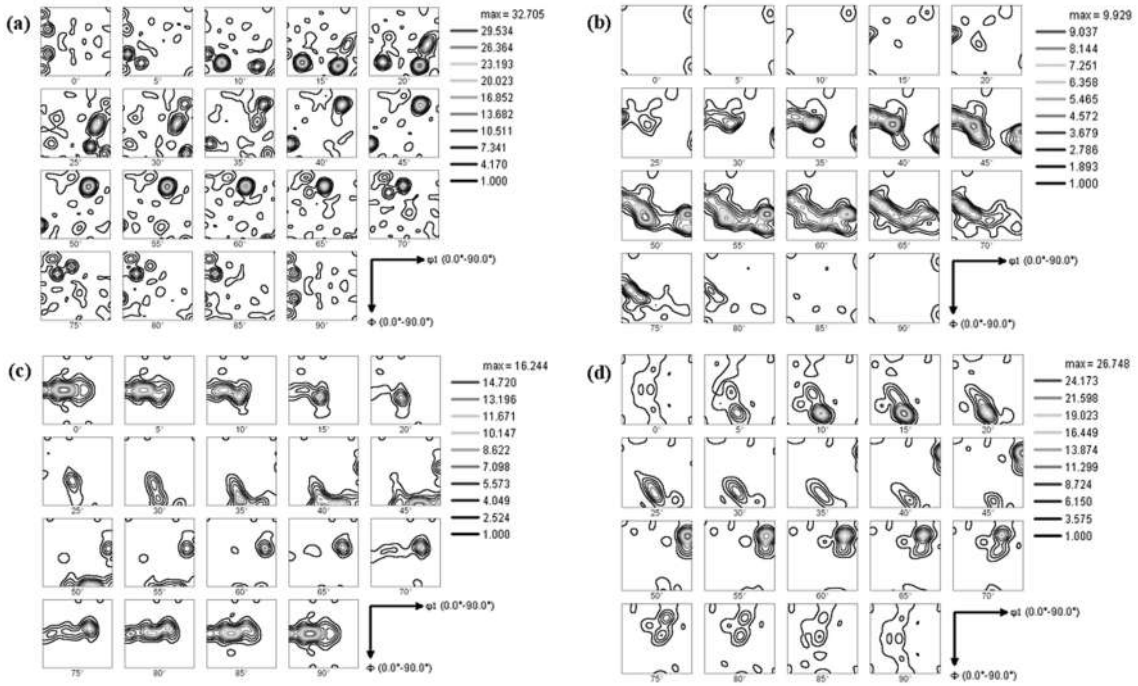

Fig. 8. ODFs of the (a) 2024 aluminum alloy and stir zone of FSW joints at (b) 500 rpm–160 mm/min, (c) 750 rpm–160 mm/min, and (d) 1000 rpm–160 mm/min.

[DOI: 10.22068/ijmse.15.1.53]

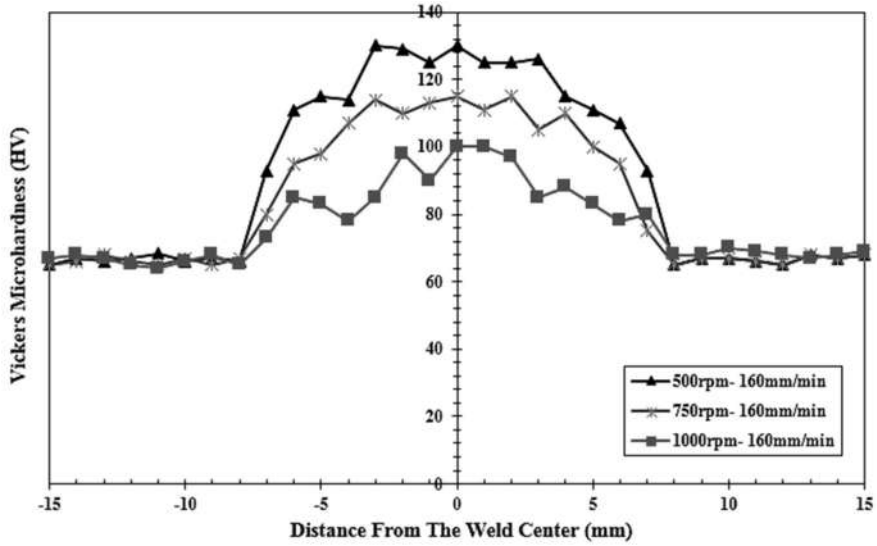

Fig. 9. Microhardness profiles along the thickness cross section of the FSW joints.

the stir zone is higher than that in the base metal in each case being due to the grain refinement [28, 29]. The hardness of the welded zone decreased from 132 to 100 HV when increasing the rotation rate from 500 to 1000 rpm. As the rotation rate increases, the heat input increases and the grain size becomes larger (Fig. 4).

The variation trend in the hardness kept pace with the change of the grain size in the SZs. According to the Hall–Petch relationship, the larger grain size results in lower hardness. Distribution and size of second phase particles in the SZs of the FSW joints were different from that in the BM [2, 4]. The average sizes of the particles in the SZs were much smaller than those in the BM. This is attributed to the breaking effect of the threaded pin in the SZ [30]. At different FSW parameters, the particles in the SZs were also different. Elangovan et al. [31] considered that at a very high rotation rate, the second phase particles could be broken up sufficiently, at the same time, the particles could be coarsened due to elevated temperature. As the rotation rate increased, the volume fraction of the coarse second phase particles decreased.

4. CONCLUSIONS

Thin 2024 aluminum alloy sheets were successfully friction stir welded under different welding conditions. The grain structure and crystallographic texture in the stir zone were investigated. The main results obtained are summarized as follows;

I. Electron back scattered diffraction (EBSD) analysis revealed that fine equiaxed grain structures in the stir zone were formed by frication stir welding process. At a constant welding speed of 160 mm/min, the size of the grains in the stir zone increased with increasing the tool rotation speed from 500 to 1000 rpm.

1. When the tool rotation speed increased, the fraction of high angle grain boundaries and the mean misorientation angle of the boundaries decreased. At a constant welding speed of 160 mm/min, the fraction of high angle grain boundaries and the mean misorientation angle of the FSW joints at 500 rpm were 63.6% and 24.96°, respectively compared with that of the FSW joints at 1000 rpm (53.6% and 17.37°, respectively).

[DOI: 10.22068/ijmse.15.1.53]

2. The recrystallization occurred in the FSW joint samples and this phenomenon led to decrease in the orientation intensities of α-fiber and τ-fiber, and the intensity of Copper {112}<111> and Goss {011}⟨100⟩ orientations remarkably increased. Also, the change in the texture well agreed with the change in the microstructure morphology.
3. With increasing the tool rotation speed, the intensity of Cube {001}<100>, Y {111}<112>, S {123}<634>, and Dillamore {4 4 11}<11 11 8> texture orientations increased and the intensity of Brass {011}<211> texture orientation decreased.
4. The FSW joints exhibited significantly hardened welded zones. As the rotation rate increased from 500 to 1000 rpm, the hardness of the stir zone decreased.

5. ACKNOWLEDGMENT

Financial support provided by Semnan University (Grant No. 266-94-3982) is gratefully acknowledged. Also, the authors wish to heartly thanks Prof. N. Tsuji of the Kyoto University, Kyoto, Japan for valuable discussion and providing equipment for EBSD analysis in Laboratory of Structure and Property of Materials of Kyoto University, Kyoto, Japan.

REFERENCES

1. Dawes, C. J, and Thomas, W. M., "Friction stir joining of aluminum alloys". TWI Bulletin, The Welding Institute, 1995, 124-127.
2. Mishra, R. S., and Ma, Z. Y., "Friction stir welding and processing". Mater. Sci. Eng. R Rep. 2005, 50(1-2), 1-78.
3. Jata, K. V., and Semiatin, S. L., "Continuous dynamic recrystallization during friction stir welding of high strength aluminum alloys". Scr Mater. 2000, 43(8), 743-749.
4. Threadgill, P. L., Leonard, A. J., Shercliff, H. R., and Withers, P. J., "Friction stir welding of aluminium alloys". Int. Mater. Rev. 2009, 54(2), 49-93.
5. Naseri, M., Reihanian, M., and Borhani, E., "Bonding behavior during cold roll-cladding of tri-layered Al/Brass/Al composite". J. Manuf. Process. 2016, 24, 125–137.
6. Scialpi, A., De Giorgi, M., De Filippis, L. A. C., Nobile, R., and Panella, F. W., "Mechanical analysis of ultra-thin friction stir welding joined sheets with dissimilar and similar materials". Mater. Des. 2008, 29(5), 928-936.
7. Cabibbo, M., McQueen, H. J., Evangelista, E., Spigarelli, S., Di Paola, M., and Falchero, A., "Microstructure and mechanical property studies of AA6056 friction stir welded plate". Mater. Sci. Eng. A. 2007, 460-461, 86-94.
8. Cho, J. H., and Dawson, P. R., "Investigation on texture evolution during friction stir welding of stainless steel". Metall. Mater. Trans. A. 2006, 37(4), 1147-1164.
9. Han, J. H., Suh, J. Y., Jee, K. K., and Lee, J. C., "Evaluation of formability and planar anisotropy based on textures in aluminum alloys processed by a shear deforming process". Mater. Sci. Eng. A. 2008, 477(1-2), 107-120.
10. Yoon, S., Ueji, R., and Fujii, H., "Effect of rotation rate on microstructure and texture evolution during friction stir welding of Ti–6Al–4V plates". Mater. Charac.2015, 106, 352-358.
11. Heidarzadeh, A., Saeid, T., and Klemm, V., "Microstructure, texture, and mechanical properties of friction stir welded commercial brass alloy". Mater. Charac.2016, 119, 84-91.
12. Babu, S., Elangovan, K., Balasubramanian, V., and Balasubramanian, M., "Optimizing friction stir welding parameters to maximize tensile strength of AA2219 aluminum alloy joints". Met. Mater. Int. 2009, 15(2), 321-330.
13. Zhang, Z., Xiao, B. L., and Ma, Z. Y., "Effect of welding parameters on microstructure and mechanical properties of friction stir welded 2219Al-T6 joints". J. Mater. Sci. 2012, 47(9), 4075-4086.
14. Suhuddin, U. F. H. R., Mironov, S., Sato, Y. S., and Kokawa, H., "Grain structure and texture evolution during friction stir welding of thin 6016 aluminum alloy sheets". Mater. Sci. Eng. A. 2010, 527(7-8), 1962-1969.
15. Zhou, L., Liu H. J., Liu, P., and Liu, Q. W., "The stir zone microstructure and its formation mechanism in Ti–6Al–4V friction stir welds".

[DOI: 10.22068/ijmse.15.1.53]

Scr Mater. 2009, 61(6), 596-599.
16. Zhou, L., Liu, H. J., and Liu, Q.. W., "Effect of rotation speed on microstructure and mechanical properties of Ti–6Al–4V friction stir welded joints'. Mater. Des. (1980-2015). 2010, 31(5), 2631-2636.
17. Mironov, S., Onuma, T., Sato, Y. S., and Kokawa, H., "Microstructure evolution during friction-stir welding of AZ31 magnesium alloy". Acta Mater. 2015, 100, 301-312.
18. Sarkar, R., Pal, T. K., and Shome, M., "Material flow and intermixing during friction stir spot welding of steel". J. Mater. Process. Technol. 2016, 227, 96-109.
19. Naseri, M., Reihanian, M., and Borhani, E., "Effect of strain path on microstructure, deformation texture and mechanical properties of nano/ultrafine grained AA1050 processed by accumulative roll bonding (ARB)". Mater. Sci. Eng. A. 2016, 673, 288-298.
20. Naseri, M., Reihanian, M., and Borhani, E., "A new strategy to simultaneous increase in the strength and ductility of AA2024 alloy via accumulative roll bonding (ARB)". Mater. Sci. Eng. A. 2016, 656, 12-20.
21. Kim, Y. G., Fujii, H., Tsumura, T., Komazaki, T., and Nakata, K., "Three defect types in friction stir welding of aluminum die casting alloy". Mater. Sci. Eng. A. 2006, 415(1-2), 250-254.
22. Jamaati, R., and Toroghinejad, M. R., "Effect of stacking fault energy on deformation texture development of nanostructured materials produced by the ARB process". Mater. Sci. Eng. A. 2014, 598, 263-276.
23. Borhani, E., Jafarian, H., Shibata, A., and Tsuji, N., "Texture evolution in Al–0.2 mass% Sc alloy during ARB process and subsequent annealing". Materials Transactions. 2012, 53(11), 1863-1869.
24. Hajizadeh, K., Tajally, M., Emadoddin, E., and Borhani, E., "Study of texture, anisotropy and formability of cartridge brass sheets". J. Alloys Compd. 2014, 588, 690-696.
25. Doherty, R. D., Hughes, D. A., Humphreys, F.. J., "Current issues in recrystallization", A review. Mater. Sci. Eng. A. 1997, 238(2), 219-274.
26. Alvand, M., Naseri, M., Borhani, E., and Abdollah-Pour, H., "Nano/ultrafine grained AA2024 alloy processed by accumulative roll bonding", A study of microstructure, deformation texture and mechanical properties. J. Alloys Compd. 2017, 712, 517-525.
27. Liu, F. C, and Nelson, T. W., "In-situ grain structure and texture evolution during friction stir welding of austenite stainless steel". Mater. Des. 2017, 115, 467-478.
28. Fattah-alhosseini, A., and Taheri, A. H., "Effect of friction stir welding on corrosion behavior of pure copper in 3.5wt.% NaCl solution". J. Manuf. Process., 2015, 20, 98-103.
29. Fattah-alhosseini, A., Vakili-azghandi, M, Sheikhi, M, and Keshavarz, M.K., "Passive and electrochemical response of friction stir processed pure Titanium". J. Alloys Compd., 2017, 704, 499-508.
30. Yang, J., Xiao, B. L., Wang, D., and Ma, Z. Y., "Effects of heat input on tensile properties and fracture behavior of friction stir welded Mg–3Al–1Zn alloy". Mater. Sci. Eng. A., 2010, 527(3), 708-714.
31. Elangovan, K., and Balasubramanian, V., "Influences of pin profile and rotational speed of the tool on the formation of friction stir processing zone in AA2219 aluminium alloy". Mater. Sci. Eng. A., 2007, 459(1-2), 7-18.

[DOI: 10.22068/ijmse.15.1.53]